

# Clustering Multivariate Time Series using Energy Distance

Richard A. Davis<sup>1</sup>, Leon Fernandes<sup>1</sup>, and Konstantinos Fokianos<sup>2</sup>

<sup>1</sup>*Department of Statistics, Columbia University*

<sup>2</sup>*Department of Mathematics and Statistics, University of Cyprus*

March 28, 2023

## Abstract

A novel methodology is proposed for clustering multivariate time series data using energy distance defined in Székely and Rizzo (2013). Specifically, a dissimilarity matrix is formed using the energy distance statistic to measure separation between the finite dimensional distributions for the component time series. Once the pairwise dissimilarity matrix is calculated, a hierarchical clustering method is then applied to obtain the dendrogram. This procedure is completely nonparametric as the dissimilarities between stationary distributions are directly calculated without making any model assumptions. In order to justify this procedure, asymptotic properties of the energy distance estimates are derived for general stationary and ergodic time series. The method is illustrated in a simulation study for various component time series that are either linear or nonlinear. Finally the methodology is applied to two examples; one involves GDP of selected countries and the other is population size of various states in the U.S.A. in the years 1900–1999.

**Keywords:** Characteristic function; clustering; dissimilarity measure; energy distance; hierarchical clustering; stationarity; time series

**Mathematics Subject Classification:** Primary 62M10, 62H30; Secondary 62H20, 62H12.

## 1 Introduction

Clustering is an important concept in statistics in which data is partitioned into groups where within each group, the data share similar characteristics. By now, there are a plethora of clustering algorithms for forming such partitions (e.g., K-means and to some extent CART). Most

of these algorithms group data according to some notion of similarity (or dissimilarity) from which the data are then clustered into various groups; see Xu and Tian (2015) for a review of such procedures. That is, the data are partitioned into the same group if each member is close to each other relative to a similarity measure. The goal of this paper is to consider clustering of the component series in a multivariate time series setting, based on energy distance (see Székely and Rizzo, 2013) applied to the joint distributions of the component time series. A key advantage of this method is that the procedure is nonparametric and based on measures of closeness of joint distributions as measured through their characteristic functions. This is in contrast to parametric procedures where the clustering is performed via the parametric fitting to some family of models or to second order properties derived from autocorrelation functions; see references below. Shumway (1982) is an early and important contribution to discriminant analysis of time series that can be viewed as a precursor to the more general approach of our paper. The characteristic function is always well defined even in cases where we deal with multivariate (not necessarily normal) distributions. Lemma 2.1 shows that calculation of a suitable distance between characteristic functions is equivalent to calculation of the Euclidean distance between observations. Therefore, applying characteristic function techniques relieves the burden of distributional assumptions (which can be quite challenging in high dimensions) and at the same time provides a computationally feasible way to implement multivariate time series clustering. Zhang and An (2018) considers clustering based on pairwise distributions via copulas. However, due to the complexity of estimating joint distributions, their method was not extended to joint distributions beyond lagged pairs of observations.

To fix ideas, consider a  $d$ -dimensional time series  $\{\mathbf{X}_t = (X_{t1}, X_{t2}, \dots, X_{td})^T, t \in \mathbb{Z}\}$  whose component series are to be clustered. Based on  $n$  consecutive observations, say  $\mathbf{X}_1, \mathbf{X}_2, \dots, \mathbf{X}_n$ , the prototypical strategy is to form a measure of dissimilarity between each pair of component series. Once a measure of dissimilarity between the component series is decided upon, then a  $d \times d$  dissimilarity matrix is computed. This matrix is then used as the input to obtain the clustering via algorithms such as K-means, fuzzy C-means, spectral clustering and hierarchical clustering. The true number of clusters, which is required for the former three methods, is typically not known *a priori*; for this reason we shall focus on hierarchical clustering. In this method each component at the initial step belongs to its own cluster; at each successive step, the most similar pairs of clusters are recursively merged. The standard algorithms that facilitate cluster merging include complete linkage, single linkage, average linkage, centroid linkage and Ward's linkage (Batagelj, 1988; James *et al.*, 2013; Murtagh and Legendre, 2014). A hierarchy

is obtained wherein the most similar components are in the same cluster and as one moves up the hierarchy, the clusters become more and more dissimilar. The hierarchy is visualized as a dendrogram and is the main output of this algorithm. Procedures such as the average silhouette width (see Kaufman and Rousseeuw, 2009) can be used to determine the final number of clusters from the dendrogram.

Various dissimilarity measures for clustering time series are catalogued in Liao (2005); Fu (2011); Montero and Vilar (2014); Aghabozorgi *et al.* (2015); Maharaj *et al.* (2019) and the references therein. Typically one considers features such as autocorrelation, partial autocorrelation, periodogram, spectral density or the copula of joint distributions—the distances between these features forms the dissimilarity measure (see Galeano and Peña, 2000; Caiado *et al.*, 2006; Díaz and Vilar, 2010; Zhang and An, 2018). Dynamic time warping (DTW) utilizes a different approach where one finds an optimal mapping such that, the paired time series under the mapping minimizes a specific distance (see Berndt and Clifford, 1994). Particularly relevant to our work is the paper of Zhang and Chen (2018), where a two dimensional version of the Kolmogorov-Smirnov statistic is used as the dissimilarity measure between distributions of lagged components. The methods mentioned so far are nonparametric, but with the exception of the copula procedure, are based primarily on second order properties of the processes. As such the “distance” employed for clustering compares moments, not distributions, as it is developed later in this article. Model based approaches typically assume the component time series are realizations of ARIMA or GARCH processes; clustering is then performed via the parametric fitting to the specified model. Examples for distances in this class include Piccolo distance, Maharaj distance and cepstral-based distance (see Piccolo, 1990; Maharaj, 2000; Kalpakis *et al.*, 2001; Savvides *et al.*, 2008). General dissimilarity measures between time series which are based on their spectral densities have been studied by Kakizawa *et al.* (1998), Taniguchi and Kakizawa (2000, Ch. 6). Given two time series with spectral density matrices  $f_i(\cdot)$ ,  $i = 1, 2$ , these authors defined a dissimilarity (or disparity) measure by

$$D_H(f_1, f_2) = \frac{1}{4\pi} \int_{-\pi}^{\pi} H(f_2^{-1}(\omega)f_1(\omega))d\omega,$$

for a suitable function  $H(\cdot)$  which has to satisfy that  $D_H(f_1, f_2) \geq 0$  and  $D_H(f_1, f_2) = 0$  when  $f_1(\omega) = f_2(\omega)$ . For instance, choosing  $H(z) = z - \log(z) - 1$ ,  $z > 0$  we have the Kullback-Leibler divergence.

In a time series setting, it is important to have dissimilarity measures that go beyond just the marginal distribution of the individual components. That is, the dissimilarity measure should be

based on the joint distributions of the individual lagged components. Specifically, for a fixed lag  $h \geq 0$ , we consider the dissimilarity between the distributions of the  $h+1$  dimensional time series  $Y_t := (X_{t,j}, X_{t+1,j}, \dots, X_{t+h,j})^T$  and  $Z_t := (X_{t,k}, X_{t+1,k}, \dots, X_{t+h,k})^T$  which will be measured through the energy distance of Székely and Rizzo (2013).

Energy distance, denoted by  $d_E(Y_1, Z_1)$ , see Section 2 for the definition, is nonnegative and has the property that  $d_E(Y_1, Z_1) = 0$  holds if and only if the joint distributions of  $Y_t$  and  $Z_t$  are the same. This property for a dissimilarity measure holds only for the copula case. We provide theoretical justification for the use of the energy distance statistic. In particular, we derive asymptotic properties for the energy distance statistic for stationary ergodic time series. Additionally, energy distance works well with heavy tailed data which is generally not the case for other dissimilarity measures. Although we assume the components are of equal length, this is only for the sake of convenience; the results of this paper can be easily extended to the situation where the lengths of the time series vary across components.

The rest of the paper is organized as follows. Section 2 defines the energy distance between any two distributions. In Section 3 we present the main theorems on consistency and characterizing limit distributions of the energy distance statistic. Section 4 discusses the multivariate time series clustering algorithm. Various clustering tasks on simulated data are considered in Section 5; we experimentally obtain and compare the performance of the proposed methodology to some competing methods. Our proposed procedure performed generally better when clustering nonlinear and multivariate VAR time series than other methods. The ACF/PACF based procedures did well when the underlying component series are well differentiated by their second order properties such as, for example, Gaussian linear models. In these situations, some of the periodogram based methods outperformed our method as did the ARMA-model based method. However, this is not too surprising since these particular procedures are tuned well for this special class of models. Further details on the simulations and performance can be found in Section 5. Two real world data sets are also considered. The first is the annual GDP data for selected countries and the second involves the population growth for a number of states in the U.S.A. in the years 1900–1999. Proofs of all the main results in this paper are deferred to the Appendix.

## 2 Energy Distance between Distributions

Before introducing energy distance, it will be helpful to first fix some notation. Throughout this paper, the inner-product between vectors  $y, z \in \mathbb{R}^p$  is denoted by  $\langle y, z \rangle = \sum_{j=1}^p y_j z_j$  and

let  $|y|^2 = \langle y, y \rangle$ . For a complex number  $z = a + ib$ , where  $i$  is the imaginary number and the complex modulus is denoted by  $|z| = \sqrt{a^2 + b^2}$ . Further, if  $X = (Y, Z)$  is a random vector then  $\dot{X} = (\dot{Y}, \dot{Z})$  and  $\ddot{X} = (\ddot{Y}, \ddot{Z})$  denote i.i.d copies of  $X$ .

Let  $Y$  and  $Z$  denote  $p$ -dimensional random vectors with characteristic functions  $\varphi_Y$  and  $\varphi_Z$  respectively. The energy distance (Székely and Rizzo, 2013) between  $Y$  and  $Z$  is defined by

$$d_E(Y, Z) := \int_{\mathbb{R}^p} |\varphi_Y(s) - \varphi_Z(s)|^2 d\mu(s), \quad (2.1)$$

where  $\mu$  is the infinite measure given by

$$d\mu(s) = \frac{ds}{|s|^{p+1} c_p}, \quad (2.2)$$

and  $c_p = \pi^{(p+1)/2} / \Gamma((p+1)/2)$ . Other weight functions can also be used; see Remark 1 for more details. The significance of using this particular weight function in evaluating (2.2) is that the integral (2.1) can be explicitly calculated, as shown in the following lemma.

**Lemma 2.1.** *Consider random vectors  $Y, Z$  in  $\mathbb{R}^p$ . If  $\mathbb{E}[|Y| + |Z|] < \infty$  then  $d_E(Y, Z) < \infty$ . Furthermore,*

$$d_E(Y, Z) = 2\mathbb{E}|Y - \dot{Z}| - \mathbb{E}|Y - \dot{Y}| - \mathbb{E}|Z - \dot{Z}|. \quad (2.3)$$

The proof is provided in the Appendix. Note that (2.3) provides a simple formula for  $d_E(Y, Z)$  and it only depends on Euclidean distances between random vectors. Lemma 2.1 implies calculation of  $d_E(Y, Z)$  requires finite first moments to guarantee finiteness of the energy distance statistic. The expression we obtain here is similar to the maximum mean discrepancy (MMD), as given by Gretton *et al.* (2012).

It is clear from (2.1) that  $d_E(Y, Z)$  is nonnegative and equality holds if and only if  $Y$  and  $Z$  have the same distribution. As mentioned earlier, this simple observation is the basis for the clustering methodology that we consider in the following section. Indeed we can obtain sample estimates for  $d_E(Y, Z)$  and then calculate a dissimilarity measure between the distributions of  $Y$  and  $Z$ ; consequently,  $d_E(Y, Z)$  can be employed for clustering. The method is completely nonparametric and easy to implement. For illustration purposes we display the theoretically calculated energy distance in the two examples below.

**Example 1.** Let  $Z \sim \mathcal{N}(0, 1)$  have a standard normal distribution. For  $t \in \mathbb{R}$  a straightforward calculation yields  $\mathbb{E}|Z - t| = |t|(2\Phi(|t|) - 1) + \sqrt{\frac{2}{\pi}}e^{-t^2/2}$ , where  $\Phi(\cdot)$  is the cdf of the standard

normal. It then follows that for any  $\theta \in \mathbb{R}$  and  $\sigma > 0$ ,

$$d_E(\sigma Z + \theta, Z) = 2\sqrt{\sigma^2 + 1} \left( |\tau| (2\Phi(|\tau|) - 1) + \sqrt{\frac{2}{\pi}} e^{-\tau^2/2} \right) - \frac{2}{\sqrt{\pi}} (\sigma + 1),$$

where  $\tau = \theta/\sqrt{\sigma^2 + 1}$ .

**Example 2.** Let  $Y \sim \mathcal{L}(0, \lambda)$  have a Laplace distribution with density  $f_Y(y) = e^{-|y|/\lambda}/(2\lambda)$ , where  $\lambda > 0$ . For  $t \in \mathbb{R}$ ,  $\mathbb{E}|Y - t| = \lambda e^{-|t|/\lambda} + |t|$ . Then,

$$d_E(Y, Z) = 4\lambda(1 - \Phi(\lambda^{-1})) \exp\left(\frac{1}{2\lambda^2}\right) - \frac{3\lambda}{2} + \frac{2(\sqrt{2} - 1)}{\sqrt{\pi}}.$$

**Remark 1.** Alternatively, consider probability measures instead of  $\mu$  in (2.2), such as a Gaussian measure; see Hong *et al.* (2017). Employing a probability measure guarantees finiteness of the integral without assuming that the random vectors  $Y$  and  $Z$  have finite means. Although we use the  $\mu$  in (2.2) associated with energy distance, similar results can be obtained with  $\mu$  replaced by a probability measure. We give a few details to be more specific: let  $d_P(Y, Z)$  denote the distance (2.1) with  $\mu$  replaced by a probability measure  $\mu_P$ . Then, easy calculations show that the counterpart of (2.3) is given by

$$d_P(Y, Z) = \mathbb{E}\text{Re}\varphi_P(Y - \dot{Y}) + \mathbb{E}\text{Re}\varphi_P(Z - \dot{Z}) - 2\mathbb{E}\text{Re}\varphi_P(Y - \dot{Z}),$$

where  $\varphi_P$  is the characteristic function of  $\mu_P$  and  $\text{Re}(\cdot)$  denotes the real part of a complex number. Hence, choosing  $\mu_P$  whose characteristic function is explicitly known yields different formulas for  $d_P(Y, Z)$ . For example if  $\mu_P$  is the Gaussian measure given by  $d\mu_P(s) = (\sqrt{2\pi\sigma^2})^{-1} \exp(-s^2/(2\sigma^2)) ds$  for  $s \in \mathbb{R}$  and some  $\sigma^2 > 0$ , then  $\text{Re}\varphi_P(s) = \exp(-\sigma^2 s^2/2)$  so that

$$d_P(Y, Z) = \mathbb{E}[\exp(-\sigma^2(Y - \dot{Y})^2/2)] + \mathbb{E}[\exp(-\sigma^2(Z - \dot{Z})^2/2)] - 2\mathbb{E}[\exp(-\sigma^2(Y - \dot{Z})^2/2)].$$

### 3 Empirical Energy Distance Statistic for Time Series

Let  $\{(Y_t, Z_t)\}$  be a stationary and ergodic time series, where  $Y_t, Z_t \in \mathbb{R}^p$ . Denote the stationary distribution of this process by  $(Y, Z)$ . We will now show how to empirically estimate  $d_E(Y, Z)$  based on observations  $(Y_1, Z_1), \dots, (Y_n, Z_n)$  using the empirical characteristic function and obtain the asymptotic properties of this estimator. Although we have assumed that the sample sizes of  $\{Y_t\}$  and  $\{Z_t\}$  are the same, this is not necessary since we are only interested estimating the marginal characteristic functions. It is straightforward to adapt our results to the case of unequal

sample sizes. Let  $\hat{\varphi}_Y(s) := \frac{1}{n} \sum_{j=1}^n e^{i\langle s, Y_j \rangle}$  and similarly define  $\hat{\varphi}_Z(s)$ . The estimate of  $d_E(Y, Z)$  is given by

$$\hat{d}_E(Y, Z) := \int_{\mathbb{R}^p} |\hat{\varphi}_Y(s) - \hat{\varphi}_Z(s)|^2 d\mu(s).$$

Leveraging (2.3) we can write  $\hat{d}_E(Y, Z)$  as the  $V$ -statistic,

$$\hat{d}_E(Y, Z) = \frac{2}{n^2} \sum_{j,k=1}^n |Y_j - Z_k| - \frac{1}{n^2} \sum_{j,k=1}^n |Y_j - Y_k| - \frac{1}{n^2} \sum_{j,k=1}^n |Z_j - Z_k|. \quad (3.1)$$

We thus have the sample estimate  $\hat{d}_E(Y, Z)$  that can be computed easily and it is based solely on the distance between the observations. Note that (3.1) is computable even in the case of multivariate observations (dependent or not). The following theorem shows that  $\hat{d}_E(Y, Z)$  is a consistent estimator for  $d_E(Y, Z)$ :

**Theorem 3.1.** *Consider stationary and ergodic time series  $\{(Y_t, Z_t)\}$ , where  $Y_t, Z_t \in \mathbb{R}^p$  and let  $(Y, Z)$  have the same distribution as  $(Y_1, Z_1)$ . Assuming  $\mathbb{E}[|Y| + |Z|] < \infty$ , we have as  $n \rightarrow \infty$*

$$\hat{d}_E(Y, Z) \xrightarrow{a.s.} d_E(Y, Z). \quad (3.2)$$

The proof is provided in the Appendix and it involves studying the asymptotic behavior of the empirical characteristic function process. To obtain the asymptotic distribution, we need additional moment assumptions and the notion of weak dependence. In what follows, assume that  $\{(Y_t, Z_t)\}$  is an  $\alpha$ -mixing time series with rate function  $\alpha(h)$ . Recall the definition of  $\alpha$ -mixing (Doukhan, 1994, p. 18): for integers  $h \geq 0$ , the  $\alpha$  mixing rate function is defined by

$$\alpha(h) = \sup |\mathbb{P}(U \cap V) - \mathbb{P}(U)\mathbb{P}(V)|,$$

where the suprema is taken over  $U \in \sigma((Y_s, Z_s), s = \dots, -1, 0)$ , and  $V \in \sigma((Y_s, Z_s), s = h+1, h+2, \dots)$ , respectively. The process is then said to be  $\alpha$ -mixing if  $\alpha(h) \rightarrow 0$  as  $h \rightarrow \infty$ . The following theorem characterizes the asymptotic distributions, whereby the rate of convergence differs according to whether or not the distributions of  $Y$  and  $Z$  are equal.

**Theorem 3.2.** *Consider stationary and ergodic time series  $\{(Y_t, Z_t)\}$  where  $Y_t, Z_t \in \mathbb{R}^p$  such that  $\sum_h \alpha(h)^{1/r} < \infty$  for some  $r > 1$ . Set  $u = 2r/(r-1)$  and write  $Y_1 = (Y_{11}, \dots, Y_{1,p})^T$  and  $Z_1 = (Z_{11}, \dots, Z_{1,p})^T$ . Assume that for some  $\alpha \in (u/2, u]$  the following hold:*

$$\mathbb{E}[|Y_1|^\alpha + |Z_1|^\alpha] < \infty \text{ and } \mathbb{E} \left[ \left( 1 \vee \prod_{\ell=1}^p |Y_{1\ell}|^\alpha \right) \left( 1 \vee \prod_{\ell=1}^p |Z_{1\ell}|^\alpha \right) \right] < \infty. \quad (3.3)$$

1. If  $Y_1$  and  $Z_1$  have the same distribution then,

$$n\hat{d}_E(Y, Z) \xrightarrow{d} \|G\|_\mu^2 = \int_{\mathbb{R}^p} |G(s)|^2 d\mu(s),$$

where  $G(s)$  is a complex-valued mean-zero Gaussian process with covariance structure for  $s, t \in \mathbb{R}^p$  given by

$$\text{Cov}(G(s), G(t)) = \sum_{h \in \mathbb{Z}} \text{Cov}(e^{i\langle s, Y_0 \rangle} - e^{i\langle s, Z_0 \rangle}, e^{i\langle t, Y_h \rangle} - e^{i\langle t, Z_h \rangle}). \quad (3.4)$$

2. If  $Y_1$  and  $Z_1$  do not have the same distribution then,

$$\sqrt{n}(\hat{d}_E(Y, Z) - d_E(Y, Z)) \xrightarrow{d} G'_\mu = \int_{\mathbb{R}^p} G'(s) d\mu(s),$$

where  $G'(s) = 2\text{Re}[(\varphi_Y(s) - \varphi_Z(s)) \cdot \overline{G(s)}]$ .

Theorems 3.1 and 3.2 state that under minimal assumptions  $\hat{d}_E(Y, Z)$  is a consistent estimator for  $d_E(Y, Z)$  and under additional moment and mixing conditions, converges in distribution, suitably normalized. The rates of convergence are different depending on whether or not  $Y$  is equal in distribution to  $Z$ . In particular, we see that  $n\hat{d}_E(Y, Z)$  converges to a non-degenerate random variable when  $Y$  and  $Z$  have the same distribution, but tends to infinity otherwise.

## 4 Multivariate Time Series Clustering

### 4.1 Dissimilarity metric based on $(h+1)$ -dimensional joint distributions

Consider observations  $\{\mathbf{X}_1, \mathbf{X}_2, \dots, \mathbf{X}_n\}$  from a multivariate time series  $\mathbf{X}_t = (X_{t1}, X_{t2}, \dots, X_{td})^T$  in  $\mathbb{R}^d$ . In this section, a general methodology for clustering component time series based on  $(h+1)$ -dimensional distributions, for a fixed lag  $h \geq 0$ , is presented. We compute a pairwise dissimilarity matrix using the energy distance on these joint distributions and then apply a hierarchical clustering algorithm to classify the data.

The dissimilarity measure based on the  $h$ -lagged  $j^{\text{th}}$  and  $k^{\text{th}}$  components of  $\mathbf{X}_t$  is given by  $D_{jk} = \hat{d}_E(Y, Z)$ , where  $Y_t = (X_{t,j}, X_{t+1,j}, \dots, X_{t+h,j})^T$  and  $Z_t = (X_{t,k}, X_{t+1,k}, \dots, X_{t+h,k})^T$  for  $t = 1, \dots, n-h$ . The energy distance dissimilarity measure is given by  $D_{jk} := \hat{d}_E(Y, Z)$ ; see also Fokianos and Pitsillou (2018). Note that  $D_{jj} = 0$  and due to symmetry,  $D_{kj} = D_{jk}$ . In this way, we form the energy distance dissimilarity matrix  $D = [D_{jk}]_{j,k=1}^p$ .

To obtain the clustering, an agglomerative hierarchical clustering method (see for example, Batagelj, 1988) is used which we briefly describe below. We start with the original  $d$  components,



as nodes, and successively merge nodes (or clusters) to form new clusters. The inter-cluster dissimilarities are then obtained as  $d(C_j, C_k) = D_{jk}$  for  $1 \leq j \neq k \leq d$ . The least dissimilar pair of components, say  $C_j$  and  $C_k$ , are now merged; note that only  $d - 1$  inter-cluster dissimilarities need to be updated. We employ the generalized Ward's linkage algorithm in this paper which has an update formula for computing the dissimilarity between the merged cluster  $C_j \cup C_k$  with  $C_\ell$  for  $\ell \neq j, k$ . This formula, known as the Lance-Williams formula for generalized Ward's linkage, is given by

$$d(C_j \cup C_k, C_\ell) = \frac{n_j + n_\ell}{n_j + n_k + n_\ell} d(C_j, C_\ell) + \frac{n_k + n_\ell}{n_j + n_k + n_\ell} d(C_k, C_\ell) - \frac{n_\ell}{n_j + n_k + n_\ell} d(C_j, C_k), \quad (4.1)$$

where  $n_i$  denotes the number of components in cluster  $C_i$ . Proceeding forward, suppose now there are  $J$  clusters  $C_1, \dots, C_J$  with a  $J \times J$  inter-cluster dissimilarity matrix  $D$ . The pair  $C_j, C_k$  with the least dissimilarity are merged with the resulting inter-cluster dissimilarities (for the  $J - 1$  clusters) are given by (4.1). The clustering algorithm is summarized in Algorithm 1.

---

**Algorithm 1** Time Series Clustering using Energy Distance

---

**Input:**  $\{\mathbf{X}_1, \mathbf{X}_2, \dots, \mathbf{X}_n\}, h$

**for**  $j < k$  where  $j, k \in \{0, 1, \dots, d\}$  **do**

$Y_t \leftarrow (X_{t,j}, X_{t+1,j}, \dots, X_{t+h,j})$

$Z_t \leftarrow (X_{t,k}, X_{t+1,k}, \dots, X_{t+h,k})$

$D_{jk} \leftarrow \hat{d}_E(Y, Z)$

**end for**

Initialize clusters  $C_1, \dots, C_d$  where  $C_j$  contains the  $j^{\text{th}}$  component time series.

Set the inter cluster dissimilarities  $d(C_j, C_k) \leftarrow D_{jk}$ ,  $1 \leq j \neq k \leq d$ .

**for**  $J = d, d - 1, \dots, 2$  **do**

Identify  $1 \leq j \neq k \leq J$  with smallest  $d(C_j, C_k)$ . Merge to form  $C_j \cup C_k$ .

Update the inter cluster dissimilarities for  $J - 1$  clusters using (4.1).

**end for**

---

If the true number of clusters ( $K_0$ ) is known, then one can obtain  $K_0$  clusters from the hierarchical clustering. As the true number of clusters are usually not known, metrics such as the average silhouette width (Kaufman and Rousseeuw, 2009) can be used to determine the final number of clusters. The silhouette coefficients are defined for each component and are based on the tightness and separation of the clusters using the dissimilarity matrix  $D$ . Specifically, if we obtain  $K$  clusters  $\{C_1, \dots, C_K\}$  from the hierarchical clustering, then the  $i^{\text{th}}$ -node silhouette

coefficient is defined as

$$s(i) = \frac{d(i, C_k) - d(i, C_j)}{\max(d(i, C_k), d(i, C_j))},$$

where  $d(i, C_\ell)$  is the average dissimilarity of component  $i$  to all components in  $C_\ell$ ,  $1 \leq \ell \leq K$ ,  $C_j$  is the cluster that contains the  $i^{\text{th}}$  component and  $C_k$  is the cluster which satisfies  $d(i, C_k) = \min_{\ell \neq j} d(i, C_\ell)$ . Clearly  $-1 \leq s(i) \leq 1$  and the closer  $s(i)$  is to one, the better the quality of the clustering. The average silhouette width is obtained as the average value of  $s(i)$  among all the  $d$  components. The average silhouette width is computed for  $K$  clusters for  $2 \leq K < d$ . The value of  $K$  which maximizes the average silhouette width is the most appropriate choice for the number of clusters.

## 4.2 Clustering via Lagged Bivariate Distributions

Instead of using  $(h+1)$ -dimensional distributions for comparison one could simplify and restrict attention to lagged bivariate distributions. More precisely, for each  $\ell \in \{1, \dots, h\}$  compute the energy distance  $D_{j,k}^{(\ell)} = \hat{d}_E(Y, Z)$ , where  $Y_t = (X_{t,j}, X_{t+\ell,j})$  and  $Z_t = (X_{t,k}, X_{t+\ell,k})$ . We also include  $D^{(0)}$ , the lag zero dissimilarity matrix which computes the pairwise dissimilarity between the marginal distributions of the components. This yields  $(h+1)$  dissimilarity matrices,  $D^{(\ell)}$  for  $\ell = 0, \dots, h$  which contain the distances between  $X_t$  and  $X_{t+\ell}$ . An overall (total) dissimilarity matrix is defined by  $D = \sum_{\ell=0}^h D^{(\ell)}$ . A similar approach can be found in Zhang and An (2018) and Zhang and Chen (2018) where a (weighted) sum of dissimilarity matrices up to some maximum lag is used as the final dissimilarity matrix. The hierarchical clustering method described Subsection 4.1 is then applied to  $D$ .

## 5 Empirical Comparisons and Applications

To assess the performance of our method we consider several simulated data sets. In addition, we apply our method to two real data sets in this section. Three clustering tasks with simulated data are considered, where for the first two, the experiments of Díaz and Vilar (2010) are performed for comparison. Next, the third simulated data set consists of clustering the components of a 40 dimensional VAR time series. The two real data sets concern the G.D.P data of the world's most developed countries between, as observed between 1990 to 2011, and the populations of a subset of states in the U.S.A. between the years of 1900 to 1999.

## 5.1 Simulation Examples

In the experiments we applied Algorithm 1 with different lags  $h = 0, 1, 2$  and  $5$ . See Remark 2 below for comments on the choice of lag  $h$ . For comparison, various competing clustering methods using different dissimilarity measures (15 in total) that have been proposed in the existing literature were considered. In the ACF based methods (see Galeano and Peña, 2000), the dissimilarity measure is equal to a geometrically downweighted distance between the estimated ACF of each pair of components. In symbols, if  $\hat{\rho}_{\ell, X_j}$  and  $\hat{\rho}_{\ell, X_k}$  represent the estimated autocorrelations of the  $j^{th}$  and  $k^{th}$  components at lag  $\ell$  respectively, then the dissimilarity measure is given by  $(\sum_{\ell=1}^L p(1-p)^\ell \cdot (\hat{\rho}_{\ell, X_j} - \hat{\rho}_{\ell, X_k})^2)^{1/2}$ , where  $L$  is the maximum lag considered and  $0 < p < 1$ . In our simulations we take  $p = 0.05$  and  $L = 10, 25, 50$ . The analogous PACF based methods are also considered wherein the estimated ACF coefficients are replaced with the corresponding estimated PACF coefficients. In the graphs displaying the results below, these procedures are labeled by *ACFLh* and *PACFLh* while the energy-based methods are labeled *EnergyLh*, where  $h$  is the lag.

We also compared these methods with periodogram-based methods of Caiado *et al.* (2006) that calculates Euclidean distances between the periodograms and log-periodograms. In addition, integrated periodogram of Casado de Lucas (2010), which computes the integral difference between the cumulative versions of the periodograms, is also included. Finally, the ARMA model based dissimilarity measures developed in Piccolo (1990) and Maharaaj (2000) were also compared. The above methods obtain different dissimilarity matrices from which hierarchical clustering is then performed using generalized Ward's method. We found that in our simulations, the clustering performance with energy distance was the highest with Ward's linkage. Other linkage algorithms with respect to competing dissimilarity measures did not have significantly different performance. These methods are labeled as *PER*, *PER.LP*, *INT.PER*, *AR.MAH*, and *AR.PIC* in the graphs below.

When the ground truth is known, we can compare the clustering methods using clustering evaluation metrics. Specifically, we consider the similarity index of Gavrilov *et al.* (2000) which is defined as

$$Sim(G, A) = \frac{1}{K} \sum_{i=1}^K \max_{1 \leq j \leq K} Sim(G_i, A_j),$$

where  $G = \{G_1, \dots, G_K\}$  is the ground truth of the  $K$  clusters,  $A = \{A_1, \dots, A_K\}$  is the clustering to be assessed, and

$$Sim(G_i, A_j) = \frac{2|G_i \cap A_j|}{|G_i| + |A_j|}.$$

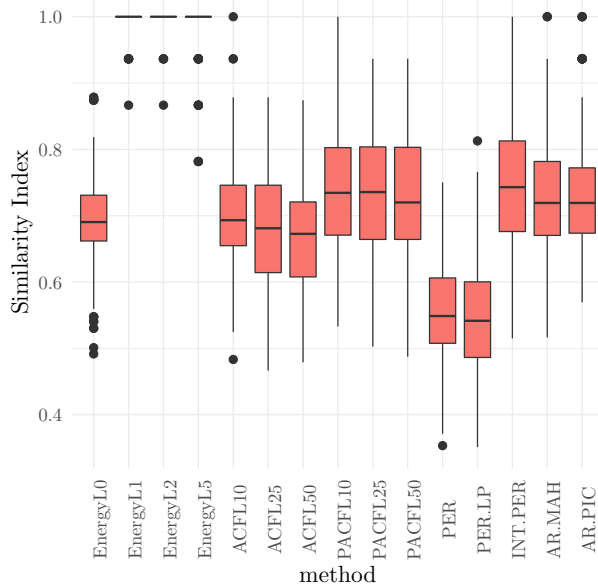


Figure 1: Comparison of similarity index of clustering methods of multivariate time series consisting of nonlinear components generated from Example 5.1. Results are based on 200 simulations and  $n = 200$ .

Here  $|\cdot|$  denotes the cardinality of a set. The similarity index takes values between 0 and 1, with 1 corresponding to perfect clustering, that is,  $G$  and  $A$  are identical. Other metrics were also considered such as the Rand index (Rand, 1971), adjusted Rand index (Hubert and Arabie, 1985) and a leave-one-out cross-validation (Tan *et al.*, 2006). However, the choice of metric did not have much impact on the relative comparisons between the various methods and we will only report the similarity index in our results.

**Example 5.1** For the first experiment, a time series consisting of 16 independent components is generated. Each component is of length  $n = 200$  and is rescaled to have mean zero and standard deviation one. We consider four clusters each of which contain four time series generated by the following models: (i) threshold autoregressive (TAR)  $X_t = 0.5X_{t-1}I(X_{t-1} \leq 0) - 2X_{t-1}I(X_{t-1} > 0) + \varepsilon_t$ , (ii) exponential autoregressive (EXPAR)  $X_t = (0.3 - 10 \exp(-X_{t-1}^2))X_{t-1} + \varepsilon_t$ , (iii) linear moving average (MA)  $X_t = \varepsilon_t - 0.4\varepsilon_{t-1}$  and (iv) nonlinear moving average (NLMA)  $X_t = \varepsilon_t - 0.5\varepsilon_{t-1} + 0.8\varepsilon_{t-1}^2$ . The sequence  $\{\varepsilon_t\}$  is assumed to be iid with a standard normal distribution in all cases. The similarity index is obtained against the ground truth of  $K_0 = 4$  clusters, for each of the 15 methods. This experiment was repeated 200 times and the boxplots

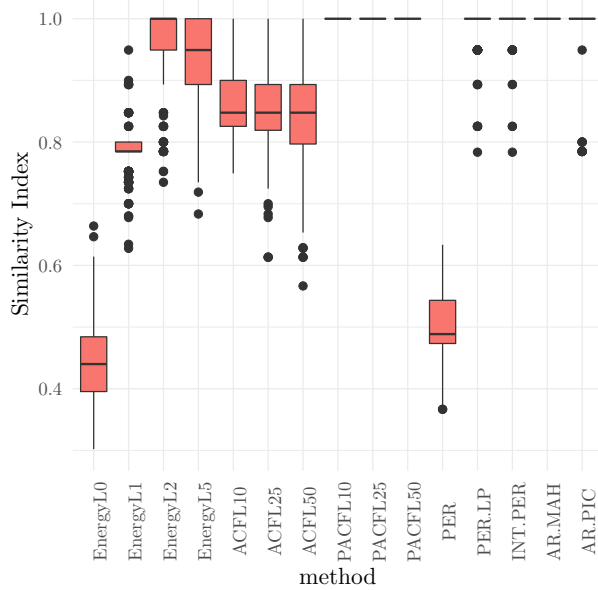


Figure 2: Comparison of similarity index of clustering methods of multivariate time series consisting of linear components generated from Example 5.2. Results are based on 200 simulations and  $n = 1000$ .

of the similarity index are shown in Figure 1. The dots in the figure denote the outliers in the boxplots. In particular, our methods with positive lags have perfect clustering in all but three instances in our experiments. It is clear that the energy distance based methods, except for lag 0, are nearly perfect in recovering the true clusters.

**Example 5.2** A very similar setup is considered in this example where we instead have five clusters, with four time series each, from the following ARMA models: (i) AR(1):  $X_t = 0.5X_{t-1} + \varepsilon_t$ , (ii) MA(1):  $X_t = 0.7\varepsilon_{t-1} + \varepsilon_t$ , (iii) AR(2):  $X_t = 0.6X_{t-1} + 0.2X_{t-2} + \varepsilon_t$ , (iv) MA(2):  $X_t = 0.8\varepsilon_{t-1} - 0.6\varepsilon_{t-2} + \varepsilon_t$ , (v) ARMA(1,1):  $X_t = 0.8X_{t-1} + \varepsilon_t + 0.2\varepsilon_{t-1}$ . The sequence  $\{\varepsilon_t\}$  is iid normally distributed. In this simulation we consider the lengths of the time series to be  $n = 1000$ . From Figure 2 we see that the best performance is achieved by  $d_{AR.MAH}$ ,  $d_{AR.PIC}$  and the PACF based methods, followed by  $d_{INT.PER}$  and  $d_{PER.LP}$ . This is due to the ARMA coefficients, PACF and log-periodograms being separated. It is not surprising that  $d_E$  with lag 0 performed the worst because all the marginal distributions were standard normal in the case. The ACF based methods performed worse because the theoretical auto-covariance coefficients are not well separated. Indeed, the true ACFs of the AR(2) and ARMA(2) considered here are

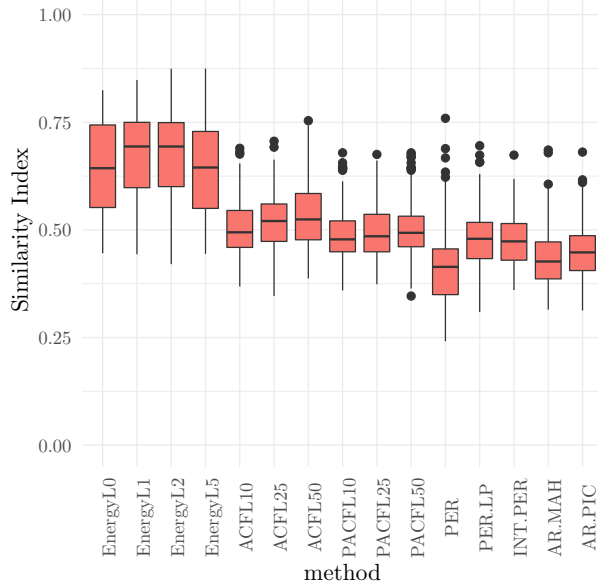


Figure 3: Comparison of similarity index of clustering methods of multivariate time series consisting of components generated from Example 5.3. Results are based on 200 simulations and  $n = 200$ .

very close to each other. Furthermore, the autocorrelation at lag 1 of the AR(1) is 0.5 and that of MA(1) is 0.47; even though the true ACF of the MA(1) process is exactly zero for higher lags while that of the AR(1) decreases geometrically by a factor of 0.5, in practice this means that the estimated ACFs of the MA(1) and AR(1) will be rather close as well. As the ACF determines the joint distributions for Gaussian ARMA time series, the energy based methods do see a reduction in performance. However, with the correct specification of the lag  $L = 2$ , we observe that the energy distance find the correct clustering most of the time.

**Example 5.3** In this example, we consider clustering a 40 dimensional time series. We generate four independent multivariate time series, each belonging to  $\mathbb{R}^{10}$  according to the following models. (i) VAR(1),  $\mathcal{N}$ :  $X_t = BX_{t-1} + \varepsilon_t$ , where the  $10 \times 10$  matrix  $B$  is constructed as 100 equally spaced numbers between  $-1$  and  $1$  column-wise which is then standardized to have spectral norm less than 1. The sequence  $\{\varepsilon_t\}$  is iid  $\mathcal{N}_{10}(\mathbf{0}, I_{10})$ . (ii) VAR(1),  $t_2$ :  $X_t = BX_{t-1} + \varepsilon_t$  where  $B$  is the same as above and the only change being that the components of  $\varepsilon_1$  are independent with a Student's t distribution with 2 degrees of freedom. (iii) VAR(2),  $\mathcal{N}$ :  $X_t = B_1X_{t-1} + B_2X_{t-2} + \varepsilon_t$ , where similar to  $B$ , the  $10 \times 10$  matrices  $B_1$  and  $B_2$  are constructed

using 100 equally spaced numbers between  $-1$  and  $0$ , and  $0$  and  $1$  respectively.  $B_1$  and  $B_2$  are standardized using the maximum eigenvalue of  $(B_1 + B_2)(B_1 + B_2)^T$ . The  $\{\varepsilon_t\}$  is iid  $\mathcal{N}_{10}(\mathbf{0}, I_{10})$ . (iv) VAR(2),  $t_2$ :  $X_t = B_1 X_{t-1} + B_2 X_{t-2} + \varepsilon_t$  with the only change being that the components of  $\varepsilon_1$  are independent and distributed as Student's  $t$  with 2 degrees of freedom. With these four underlying clusters, the clustering performance with respect to similarity index is shown in Figure 3. Our proposed method outperformed all the competing methods. The clustering performance was nearly the same for the energy distance based method for lags  $h = 0, 1, 2, 5$ . This suggests that components with the same marginal distributions have been clustered correctly and inclusion of further lagged joint distributions did not appreciably improve clustering performance.

**Remark 2.** In applications we need to decide on a suitable choice for  $h$ , the size of the joint distributions used for clustering. If there is clustering at lag  $h = 0$ , then one would expect clustering to also be present at lags  $h > 0$ . However, the nature of the clustering could be different as a function of lag. For instance there might be strong associations or disassociation in the component time series at lag 3 which is not so evident at lags 0–2. The other hurdle is that as the lag increases, the dissimilarity measure may incur more noise and hence less useful for providing meaningful clusters. On the other hand, for  $h$  small, there may not be much power in discriminating the individual time series. To some extent, this sort of behavior is manifested in Figures 2 and 3. In the case  $h = 0$  our proposed clustering procedure does a reasonably good job in correctly identifying the clusters. This performance is only improved as one uses  $h = 1$  and  $h = 2$ . However, for  $h = 5$  there is a slight falloff in the performance of the clustering. The idea of choosing an *optimal*  $h$  will be the subject of a future investigation.

## 5.2 Real Data Examples

### Application to annual G.D.P. data

In this example, we considered the annual real gross domestic product (GDP) data obtained from <https://www.conference-board.org/us/>, which was also studied in Zhang and An (2018). A set of 23 of the most developed countries in the world was used for the years 1980–2019: Austria, Belgium, Denmark, Finland, France, Germany, Greece, Iceland, Ireland, Italy, Luxembourg, the Netherlands, Norway, Portugal, Spain, Sweden, Switzerland, United Kingdom, Canada, United States, Australia, New Zealand and Japan. In total this is a 23 dimensional time series with  $n = 39$  observations each. We used the annual log growth rate, calculated for the  $j^{th}$  country

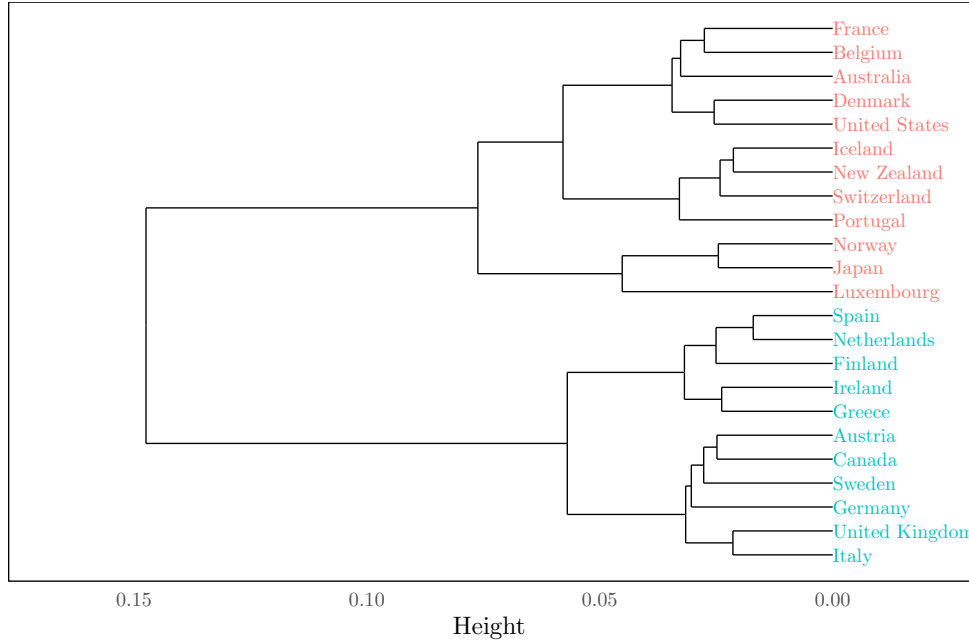


Figure 4: Clustering dendrogram obtained from real GDP data with energy distance using lag 1. The colors correspond to the final clustering based the highest average silhouette width of 0.29 obtained with 2 clusters.

as  $\log(GDP_{t,j}) - \log(GDP_{t-1,j})$  as the input time series. Each components was re-normalized to have mean zero and standard deviation one. Energy distance with lag 1 is applied to this dataset; higher values of lag did not work well due to  $n = 39$  being too small.

In this case, the maximum average silhouette width was obtained with 2 clusters and is shown in Figure 4. Figure 5 presents the the clustering on a world map. Spain, Netherlands, Finland, Ireland, Greece, Austria, Canada, Sweden, Germany, United Kingdom and Italy form the blue cluster. This cluster consists of most mainland European countries and includes the United Kingdom, Ireland and Canada. The red cluster consisted of France, Belgium, Australia, Denmark, United States, Ireland, Iceland, New Zealand, Switzerland, Portugal, Norway, Japan and Luxembourg. A possible interpretation of this result is that the blue group includes countries that spend a considerable amount of their budget on safety net programs when compared to most of the countries in the red cluster.



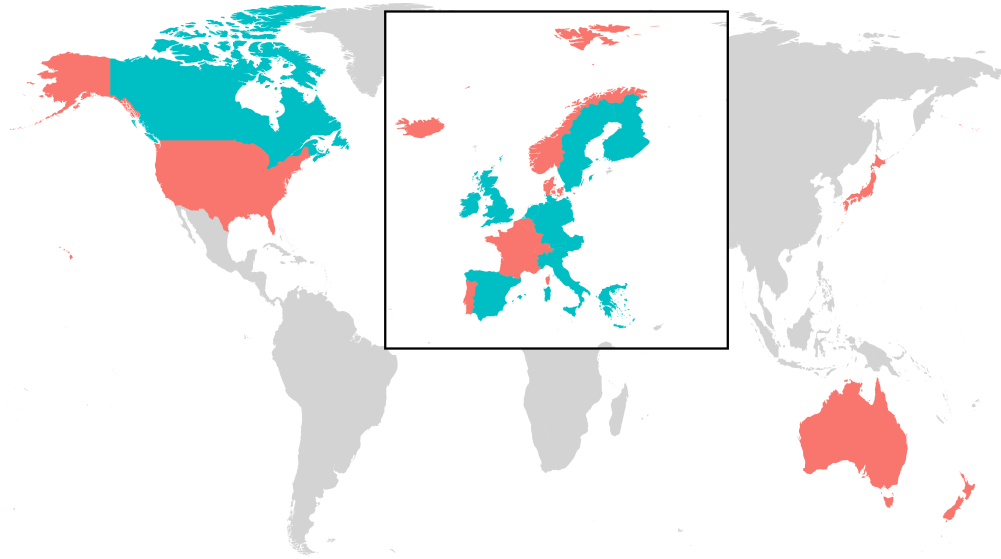


Figure 5: Clustering obtained from real GDP data using energy distance with lag 1 on a world map with a zoomed in Europe.

### U.S.A. Population Data

Consider the population of twenty states in the U.S.A. between the years of 1900–1999. This dataset, with dimension 20 and length  $n = 99$ , was studied in Kalpakis *et al.* (2001); Zhang and An (2018); Zhang and Chen (2018) and is made available from <https://www.csee.umbc.edu/kalpakis/TS-mining/ts-datasets.html>. Kalpakis *et al.* (2001) identified two clusters, where one set of states had an exponentially increasing trend whereas the second set of states had a stabilizing trend. The states in the first cluster were California, Colorado, Florida, Georgia, Maryland, North Carolina, South Carolina, Tennessee, Texas, Virginia and Washington. The latter cluster consisted of Illinois, Massachusetts, Michigan, New Jersey, New York, Oklahoma, Pennsylvania, North Dakota and South Dakota. The raw data was used to calculate the log growth rate for each state, that is,  $\log(P_{t,j}) - \log(P_{t-1,j})$ , where  $P_{t,j}$  is the population of state  $j$  at time  $t$ . Each of the time series were normalized to have zero mean and unit standard deviation. The results of clustering with  $h = 1$  are shown in Figure 6; the corresponding map of the U.S.A. is displayed in Figure 7. In this example the clustering was remarkably consistent when  $h$  varied from 0 to 5. This suggests that the stationary distributions differ between clusters. The average silhouette score suggest three clusters in this case. California, Colorado, Florida, Georgia, Maryland, Virginia, Washington, Illinois and Massachusetts are included in the red cluster and all but the

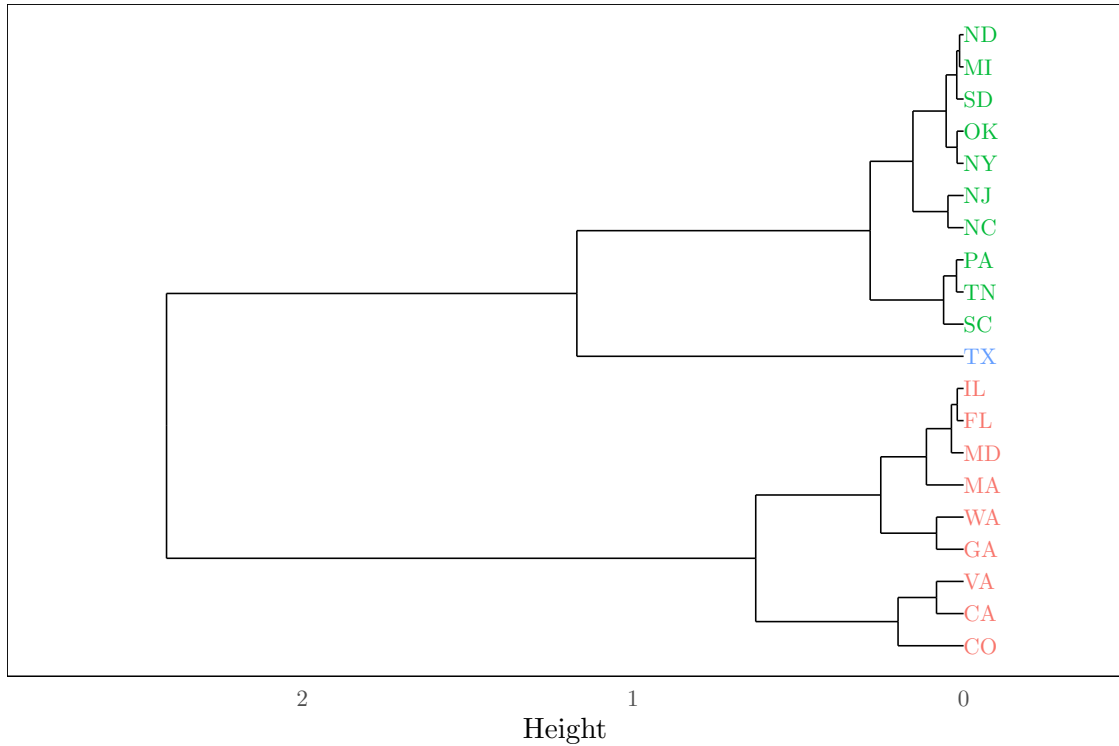


Figure 6: Clustering dendrogram obtained from population data using energy distance with lag 1. The colors correspond to the final clustering based the highest average silhouette width of 0.7 obtained with 3 clusters.

last two have exponentially increasing trends. North Carolina, South Carolina and Tennessee however were assigned to the green cluster. Texas forms it's own separate cluster; the population growth data of Texas has different distribution compared to all the other states in this experiment. The trend based clustering assignments of Kalpakis *et al.* (2001) are partially recovered and our method identifies the differences in the underlying (lagged) stationary distributions among the obtained clusters.

## Acknowledgements

The research of R. A. Davis was supported in part by NSF grant DMS 2015379 to Columbia University. We acknowledge computing resources from Columbia University's Shared Research

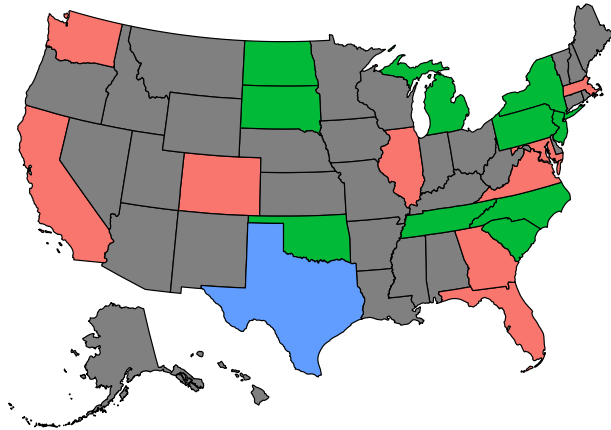


Figure 7: Clustering obtained from population data using energy distance with lag 1 on a map of the U.S.A. in the years 1900–1999.

Computing Facility project, which is supported by NIH Research Facility Improvement Grant 1G20RR030893-01, and associated funds from the New York State Empire State Development, Division of Science Technology and Innovation (NYSTAR) Contract C090171, both awarded April 15, 2010. We also thank the referees for their helpful remarks which led to a greatly improved exposition.

## References

- Aaronson J, Burton R, Dehling H, Gilat D, Hill T, Weiss B. 1996. Strong laws for  $L$ - and  $U$ -statistics. *Transactions of the American Mathematical Society*, **348**(7):2845–2866.
- Aghabozorgi S, Shirkhorshidi AS, Wah TY. 2015. Time-series clustering—a decade review. *Information systems*, **53**:16–38.
- Batagelj V. 1988. Generalized Ward and Related Clustering Problems. *Classification and Related Methods of Data Analysis*, **30**:67–74.
- Berndt DJ, Clifford J. 1994. Using Dynamic Time Warping to Find Patterns in Time Series. In *Proceedings of the 3rd International Conference on Knowledge Discovery and Data Mining, AAAIWS'94*, 359–370. AAAI Press.
- Caiado J, Crato N, Peña D. 2006. A periodogram-based metric for time series classification. *Computational Statistics & Data Analysis*, **50**(10):2668–2684.
- Casado de Lucas D. 2010. *Classification techniques for time series and functional data*. Ph.D. thesis, Universidad Carlos III de Madrid.
- Davis RA, Matsui M, Mikosch T, Wan P. 2018. Applications of distance correlation to time series. *Bernoulli*, **24**(4A):3087–3116.
- Díaz SP, Vilar JA. 2010. Comparing several parametric and nonparametric approaches to time series clustering: a simulation study. *Journal of Classification*, **27**(3):333–362.
- Doukhan P. 1994. *Mixing*, volume 85 of *Lecture Notes in Statistics*. New York: Springer-Verlag.
- Fokianos K, Pitsillou M. 2018. Testing independence for multivariate time series via the auto-distance correlation matrix. *Biometrika*, **105**:337–352.
- Fu TC. 2011. A review on time series data mining. *Engineering Applications of Artificial Intelligence*, **24**(1):164–181.
- Galeano P, Peña D. 2000. Multivariate analysis in vector time series. *Resenhas do Instituto de Matemática e Estatística da Universidade de São Paulo*, **4**(4):383–403.
- Gavrilov M, Anguelov D, Indyk P, Motwani R. 2000. Mining the stock market (extended abstract) which measure is best? In *Proceedings of the sixth ACM SIGKDD International Conference on Knowledge Discovery and Data Mining*, 487–496.

- Gretton A, Borgwardt KM, Rasch MJ, Schölkopf B, Smola A. 2012. A kernel two-sample test. *The Journal of Machine Learning Research*, **13**(1):723–773.
- Hong D, Gu Q, Whitehouse K. 2017. High-dimensional time series clustering via cross-predictability. In *Artificial Intelligence and Statistics*, 642–651. PMLR.
- Hubert L, Arabie P. 1985. Comparing partitions. *Journal of Classification*, **2**(1):193–218.
- James G, Witten D, Hastie T, Tibshirani R. 2013. *An Introduction to Statistical Learning*. New York: Springer.
- Kakizawa Y, Shumway RH, Taniguchi M. 1998. Discrimination and clustering for multivariate time series. *Journal of the American Statistical Association*, **93**:328–340.
- Kalpakis K, Gada D, Puttagunta V. 2001. Distance measures for effective clustering of ARIMA time-series. In *Proceedings 2001 IEEE International Conference on Data Mining*, 273–280. IEEE.
- Kaufman L, Rousseeuw PJ. 2009. *Finding Groups in Data: An Introduction to Cluster Analysis*. New York: Wiley.
- Krengel U. 1985. *Ergodic Theorems*. Berlin: Walter de Gruyter & Co.
- Liao TW. 2005. Clustering of time series data—a survey. *Pattern Recognition*, **38**(11):1857–1874.
- Maharaj EA. 2000. Cluster of Time Series. *Journal of Classification*, **17**(2):297–314.
- Maharaj EA, D’Urso P, Caido J. 2019. *Time Series Clustering and Classification*. Computer Science and Data Analysis. Australia: CRC Press.
- Montero P, Vilar JA. 2014. TSclust: An R Package for Time Series Clustering. *Journal of Statistical Software*, **62**(1):1–43.
- Murtagh F, Legendre P. 2014. Ward’s Hierarchical Agglomerative Clustering Method: Which Algorithms Implement Ward’s Criterion? *Journal of Classification*, **31**(3):274–295.
- Piccolo D. 1990. A distance measure for classifying ARIMA models. *Journal of Time Series Analysis*, **11**(2):153–164.
- Rand WM. 1971. Objective criteria for the evaluation of clustering methods. *Journal of the American Statistical Association*, **66**(336):846–850.

- Savvides A, Promponas VJ, Fokianos K. 2008. Clustering of biological time series by cepstral coefficients based distances. *Pattern Recognition*, **41**(7):2398–2412.
- Shumway RH. 1982. Discriminant analysis for time series. In *Classification, pattern recognition and reduction of dimensionality*, volume 2 of *Handbook of Statistics*, 1–46. Amsterdam: North-Holland.
- Stout WF. 1974. *Almost sure convergence*. New York-London: Academic Press.
- Székely GJ, Rizzo ML. 2013. Energy statistics: A class of statistics based on distances. *Journal of Statistical Planning and Inference*, **143**(8):1249–1272.
- Székely GJ, Rizzo ML, Bakirov NK. 2007. Measuring and testing dependence by correlation of distances. *The Annals of Statistics*, **35**(6):2769–2794.
- Tan PN, Steinbach M, Kumar V. 2006. *Data Mining Introduction*. Boston: Pearson Addison Wesley.
- Taniguchi M, Kakizawa Y. 2000. *Asymptotic Theory of Statistical Inference for Time Series*. New York: Springer.
- Xu D, Tian Y. 2015. A comprehensive survey of clustering algorithms. *Annals of Data Science*, **2**(2):165–193.
- Zhang B, An B. 2018. Clustering time series based on dependence structure. *PLoS ONE*, **13**(11):1–22.
- Zhang B, Chen R. 2018. Nonlinear Time Series Clustering Based on Kolmogorov-Smirnov 2D Statistic. *Journal of Classification*, **35**(3):394–421.

## A Appendices

### A.1 Proof of Lemma 2.1

From Lemma 1 in Székely *et al.* (2007), for  $x \in \mathbb{R}^p$

$$\int_{\mathbb{R}^p} \frac{1 - \cos\langle s, x \rangle}{|s|^{p+1} c_p} ds = |x|. \quad (\text{A.1})$$

Let  $(\dot{Y}, \dot{Z})$  be an independent copy of  $(Y, Z)$ . For  $s \in \mathbb{R}^p$ ,

$$\begin{aligned}
|\varphi_Y(s) - \varphi_Z(s)|^2 &= |\varphi_Y(s)|^2 + |\varphi_Z(s)|^2 - \varphi_Y(s)\overline{\varphi_Z(s)} - \overline{\varphi_Y(s)}\varphi_Z(s) \\
&= \mathbb{E}e^{i\langle s, Y - \dot{Y} \rangle} + \mathbb{E}e^{i\langle s, Z - \dot{Z} \rangle} - \mathbb{E}e^{i\langle s, Y - \dot{Z} \rangle} - \mathbb{E}e^{i\langle s, \dot{Z} - Y \rangle} \\
&= \mathbb{E}(\cos\langle s, Y - \dot{Y} \rangle) + \mathbb{E}(\cos\langle s, Z - \dot{Z} \rangle) - 2\mathbb{E}(\cos\langle s, Y - \dot{Z} \rangle) \\
&= 2\mathbb{E}(1 - \cos\langle s, Y - \dot{Z} \rangle) - \mathbb{E}(1 - \cos\langle s, Y - \dot{Y} \rangle) - \mathbb{E}(1 - \cos\langle s, Z - \dot{Z} \rangle).
\end{aligned}$$

Since  $\mathbb{E}[|Y| + |Z|] < \infty$ , we can apply Fubini's theorem and (A.1) to deduce  $d_E(Y, Z) < \infty$  and obtain (2.3).

## A.2 Proof of Theorem 3.1

We follow the steps from the proofs of Theorem 3.1 in Davis *et al.* (2018) and Theorem 2 in Székely *et al.* (2007). Accordingly, for  $\delta > 0$  we set

$$K_\delta = \{s \in \mathbb{R}^p : \delta \leq |s| \leq 1/\delta\}. \quad (\text{A.2})$$

The processes  $\hat{\varphi}_Y$  and  $\hat{\varphi}_Z$  are sample means of i.i.d bounded processes. By the ergodic theorem (Theorem 3.5.7 in Stout (1974))  $\hat{\varphi}_Y \xrightarrow{a.s.} \varphi_Y$  and  $\hat{\varphi}_Z \xrightarrow{a.s.} \varphi_Z$  on  $\mathcal{C}(K_\delta)$ , the space of continuous functions on  $K_\delta$ ; see Krengel (1985). So,

$$\int_{K_\delta} |\hat{\varphi}_Y(s) - \hat{\varphi}_Z(s)|^2 d\mu(s) \xrightarrow{a.s.} \int_{K_\delta} |\varphi_Y(s) - \varphi_Z(s)|^2 d\mu(s).$$

Thus it suffices to show

$$\lim_{\delta \downarrow 0} \limsup_{n \rightarrow \infty} \int_{K_\delta^c} |\hat{\varphi}_Y(s) - \hat{\varphi}_Z(s)|^2 d\mu(s) \xrightarrow{a.s.} 0. \quad (\text{A.3})$$

First, since  $|\hat{\varphi}_Y(s) - \hat{\varphi}_Z(s)|^2 \leq 4$  we have almost surely

$$\lim_{\delta \downarrow 0} \limsup_{n \rightarrow \infty} \int_{|s| > 1/\delta} |\hat{\varphi}_Y(s) - \hat{\varphi}_Z(s)|^2 d\mu(s) \leq 4 \lim_{\delta \downarrow 0} \int_{|s| > 1/\delta} d\mu(s) = 0.$$

Fix  $\delta > 0$ . From the proof of Lemma 2.1, we rewrite

$$\begin{aligned}
\int_{|s| < \delta} |\hat{\varphi}_Y(s) - \hat{\varphi}_Z(s)|^2 d\mu(s) &= \int_{|s| < \delta} \left[ \frac{2}{n^2} \sum_{j,k=1}^n (1 - \cos\langle s, Y_j - Z_k \rangle) \right] d\mu(s) \\
&\quad - \int_{|s| < \delta} \left[ \frac{1}{n^2} \sum_{j,k=1}^n (1 - \cos\langle s, Y_j - Y_k \rangle) \right] d\mu(s) \\
&\quad - \int_{|s| < \delta} \left[ \frac{1}{n^2} \sum_{j,k=1}^n (1 - \cos\langle s, Z_j - Z_k \rangle) \right] d\mu(s).
\end{aligned}$$

Let  $g(x) := \int_{|s| < x} (1 - \cos(s_1)) \frac{ds}{c_p s^2}$ , where  $s_1$  is the first component of  $s \in \mathbb{R}^p$ . Due to a change of variables,

$$\begin{aligned} \int_{|s| < \delta} |\hat{\varphi}_Y(s) - \hat{\varphi}_Z(s)|^2 d\mu(s) &= \frac{2}{n^2} \sum_{j,k=1}^n g(|Y_j - Z_k| \delta) |Y_j - Z_k| \\ &\quad - \frac{1}{n^2} \sum_{j,k=1}^n g(|Y_j - Y_k| \delta) |Y_j - Y_k| \\ &\quad - \frac{1}{n^2} \sum_{j,k=1}^n g(|Z_j - Z_k| \delta) |Z_j - Z_k|. \end{aligned}$$

Applying the ergodic theorem for U-statistics according to Aaronson *et al.* (1996), as  $n \rightarrow \infty$

$$\begin{aligned} \int_{|s| < \delta} |\hat{\varphi}_Y(s) - \hat{\varphi}_Z(s)|^2 d\mu(s) &\xrightarrow{a.s.} 2\mathbb{E}[g(|Y - Z| \delta) |Y - Z|] - \mathbb{E}[g(|Y - \dot{Y}| \delta) |Y - \dot{Y}|] \\ &\quad - \mathbb{E}[g(|Z - \dot{Z}| \delta) |Z - \dot{Z}|]. \end{aligned}$$

Using the continuity of  $g(\cdot)$  at zero we see  $\lim_{\delta \downarrow 0} \mathbb{E}[g(|Y - Z| \delta) |Y - Z|] = 0$  via dominated convergence. Similarly for the remaining two terms. It then follows that almost surely,

$$\lim_{\delta \downarrow 0} \limsup_{n \rightarrow \infty} \int_{|s| < \delta} |\hat{\varphi}_Y(s) - \hat{\varphi}_Z(s)|^2 d\mu(s) = 0.$$

Hence (A.3) holds, which concludes the proof.

### A.3 Proof of Theorem 3.2

In the proof below, the symbol  $c$  will denote a positive constant, whose value might change from line to line but it is not of particular interest. For  $s \in \mathbb{R}^p$ , due to stationarity of  $\{Y_t\}$ ,

$$\mathbb{E} \left[ \left| \frac{1}{n} \sum_{j=1}^n (e^{i\langle s, Y_j \rangle} - \varphi_Y(s)) \right|^2 \right] = \frac{1}{n} \sum_{h=1-n}^{n-1} (1 - |h|/n) \operatorname{Re} [\operatorname{Cov}(e^{i\langle s, Y_0 \rangle} - \varphi_Y(s), e^{i\langle s, Y_h \rangle} - \varphi_Y(s))].$$

An application of Theorem 3(a) of Section 1.2.2 in Doukhan (1994) yields

$$\begin{aligned} |\operatorname{Re} [\operatorname{Cov}(e^{i\langle s, Y_0 \rangle} - \varphi_Y(s), e^{i\langle s, Y_h \rangle} - \varphi_Y(s))]| &\leq c \alpha_h^{1/r} (\mathbb{E}[|e^{i\langle s, Y \rangle} - \varphi_Y(s)|^u])^{2/u} \\ &\leq c \alpha_h^{1/r} (\mathbb{E}[|e^{i\langle s, Y \rangle} - \varphi_Y(s)|^2])^{2/u}. \end{aligned}$$

Then, for  $\alpha \in (0, 2]$

$$\mathbb{E}[|e^{i\langle s, Y \rangle} - \varphi_Y(s)|^2] = 1 - |\varphi_Y(s)|^2 \leq \mathbb{E}[1 \wedge |\langle s, Y - \dot{Y} \rangle|^\alpha] \leq c(1 \wedge |s|^\alpha).$$



Due to the summability assumption  $\sum_h \alpha_h^{1/r} < \infty$ ,

$$\begin{aligned} n\mathbb{E}[|\hat{\varphi}_Y(s) - \varphi_Y(s)|^2] &\leq c(1 \wedge |s|^{2\alpha/u}) \sum_{h=1-n}^{n-1} (1 - |h|/n)\alpha_h^{1/r} \\ &\leq c(1 \wedge |s|^{2\alpha/u}). \end{aligned}$$

Similarly,  $n\mathbb{E}[|\hat{\varphi}_Z(s) - \varphi_Z(s)|^2] \leq c(1 \wedge |s|^{2\alpha/u})$ . It then follows that

$$\mathbb{E}[\hat{G}(s)^2] \leq c(1 \wedge |s|^{2\alpha/u}), \quad (\text{A.4})$$

where  $\hat{G}(s) := \sqrt{n}((\hat{\varphi}_Y(s) - \varphi_Y(s)) - (\hat{\varphi}_Z(s) - \varphi_Z(s)))$ . The proof of the theorem will rely on Lemma A.1(2) of Davis *et al.* (2018) stated below.

**Lemma A.1.** *Assume that  $\sum_h \alpha_h^{1/r} < \infty$  for some  $r > 1$  and set  $u = 2r/(r-1)$ . If the moment conditions (3.3) are satisfied with  $u/2 < \alpha \leq u$ , then  $\sqrt{n}(\hat{\varphi}_{Y,Z} - \varphi_{Y,Z}) \xrightarrow{d} G_{Y,Z}$  on compact sets  $K \subset \mathbb{R}^{2p}$  for some complex-valued mean-zero Gaussian field  $G_{Y,Z}$  with covariance structure*

$$\text{Cov}(G_{Y,Z}(s), G_{Y,Z}(t)) = \sum_{h \in \mathbb{Z}} \text{Cov}(e^{i\langle s, Y_0 \rangle + i\langle t, Z_0 \rangle}, e^{i\langle s, Y_h \rangle + i\langle t, Z_h \rangle}).$$

Due to Lemma A.1, on compact sets  $\sqrt{n}(\hat{\varphi}_{Y,Z} - \varphi_{Y,Z}) \xrightarrow{d} G_{Y,Z}$ . But  $\hat{G}(s) = \sqrt{n}(\hat{\varphi}_{Y,Z}(s, 0) - \varphi_{Y,Z}(0, s))$ . So on the compact set  $K_\delta$  defined in (A.2) for some  $\delta > 0$ , we obtain  $\hat{G} \xrightarrow{d} G$ , where  $G$  is a complex-valued mean-zero Gaussian process. The covariance structure is then given by

$$\begin{aligned} \text{Cov}(G(s), G(t)) &= \text{Cov}(G_{Y,Z}(s, 0) - G_{Y,Z}(0, s), G_{Y,Z}(t, 0) - G_{Y,Z}(0, t)) \\ &= \text{Cov}(G_{Y,Z}(s, 0), G_{Y,Z}(t, 0)) - \text{Cov}(G_{Y,Z}(s, 0), G_{Y,Z}(0, t)) \\ &\quad - \text{Cov}(G_{Y,Z}(0, s), G_{Y,Z}(t, 0)) + \text{Cov}(G_{Y,Z}(0, s), G_{Y,Z}(0, t)) \\ &= \sum_{h \in \mathbb{Z}} (\text{Cov}(e^{i\langle s, X_0 \rangle}, e^{i\langle t, X_h \rangle}) - \text{Cov}(e^{i\langle s, X_0 \rangle}, e^{i\langle t, Y_h \rangle}) \\ &\quad - \text{Cov}(e^{i\langle s, Y_0 \rangle}, e^{i\langle t, X_h \rangle}) + \text{Cov}(e^{i\langle s, Y_0 \rangle}, e^{i\langle t, Y_h \rangle})) \\ &= \sum_{h \in \mathbb{Z}} \text{Cov}(e^{i\langle s, X_0 \rangle} - e^{i\langle s, Y_0 \rangle}, e^{i\langle s, Y_0 \rangle} - e^{i\langle s, Y_h \rangle}). \end{aligned}$$

**Proof of Theorem 3.2(i).** If  $Y \stackrel{d}{=} Z$ , then  $\varphi_Y = \varphi_Z$  so that  $\sqrt{n}(\hat{\varphi}_Y - \hat{\varphi}_Z) \xrightarrow{d} G$  on  $K_\delta$ . By the continuous mapping theorem,

$$\int_{K_\delta} |\sqrt{n}(\hat{\varphi}_Y(s) - \hat{\varphi}_Z(s))|^2 d\mu(s) \xrightarrow{d} \int_{K_\delta} |G(s)|^2 d\mu(s).$$

Let  $\varepsilon > 0$ . From Markov's inequality, dominated convergence and (A.4),

$$\begin{aligned} & \lim_{\delta \downarrow 0} \limsup_{n \rightarrow \infty} \mathbb{P} \left( \int_{K_\delta^c} \left| \sqrt{n} (\hat{\varphi}_Y(s) - \hat{\varphi}_Z(s)) \right|^2 d\mu(s) > \varepsilon \right) \\ & \leq \varepsilon^{-1} \lim_{\delta \downarrow 0} \limsup_{n \rightarrow \infty} \int_{K_\delta^c} n \mathbb{E} \left[ \left| \hat{\varphi}_Y(s) - \hat{\varphi}_Z(s) \right|^2 \right] d\mu(s) \\ & \leq c\varepsilon^{-1} \lim_{\delta \downarrow 0} \int_{K_\delta^c} (1 \wedge |s|^{2\alpha/u}) d\mu(s) = 0. \end{aligned}$$

□

**Proof of Theorem 3.2(ii).** Now  $Y$  and  $Z$  have different distributions. Note that

$$\sqrt{n} (|\hat{\varphi}_Y(s) - \hat{\varphi}_Z(s)|^2 - |\varphi_Y(s) - \varphi_Z(s)|^2) = \hat{G}(s)(\hat{\varphi}_Y(-s) - \hat{\varphi}_Z(-s)) + \hat{G}(-s)(\varphi_Y(s) - \varphi_Z(s)).$$

From the almost sure convergence of  $\hat{\varphi}_Y(\cdot) - \hat{\varphi}_Z(\cdot)$  on compact sets and the continuous mapping theorem,

$$\sqrt{n} \int_{K_\delta} (|\hat{\varphi}_Y(s) - \hat{\varphi}_Z(s)|^2 - |\varphi_Y(s) - \varphi_Z(s)|^2) d\mu(s) \xrightarrow{d} \int_{K_\delta} G'(s) d\mu(s),$$

where  $G'(s) = 2\text{Re}[(\varphi_Y(s) - \varphi_Z(s)) \cdot \overline{G(s)}]$ . Note that for complex numbers  $z_1, z_2$  we have

$$||z_1|^2 - |z_2|^2| \leq |\text{Re}(z_1 - z_2)(\overline{z_1} + \overline{z_2})|.$$

Using this for  $z_1 = \hat{\varphi}_Y(s) - \hat{\varphi}_Z(s)$  and  $z_2 = \varphi_Y(s) - \varphi_Z(s)$ ,

$$||\hat{\varphi}_Y(s) - \hat{\varphi}_Z(s)|^2 - |\varphi_Y(s) - \varphi_Z(s)|^2| \leq c |(\hat{\varphi}_Y(s) - \hat{\varphi}_Z(s)) - (\varphi_Y(s) - \varphi_Z(s))|.$$

Therefore, by Markov's inequality, Jensen's inequality, the dominated convergence theorem and (A.4), for any given  $\varepsilon > 0$ ,

$$\begin{aligned} & \lim_{\delta \downarrow 0} \limsup_{n \rightarrow \infty} \mathbb{P} \left( \int_{K_\delta^c} \sqrt{n} \left| |\hat{\varphi}_Y(s) - \hat{\varphi}_Z(s)|^2 - |\varphi_Y(s) - \varphi_Z(s)|^2 \right| d\mu(s) > \varepsilon \right) \\ & \leq c \lim_{\delta \downarrow 0} \limsup_{n \rightarrow \infty} \int_{K_\delta^c} \sqrt{n} \mathbb{E} |(\hat{\varphi}_Y(s) - \hat{\varphi}_Z(s)) - (\varphi_Y(s) - \varphi_Z(s))| d\mu(s) \\ & \leq c \lim_{\delta \downarrow 0} \limsup_{n \rightarrow \infty} \int_{K_\delta^c} (\mathbb{E} \hat{G}(s)^2)^{1/2} d\mu(s) \\ & \leq c \lim_{\delta \downarrow 0} \int_{K_\delta^c} (1 \wedge |s|^{2\alpha/u}) d\mu(s) = 0. \end{aligned}$$

□